Molecular characterization of the interaction between human IgG and the M-related proteins from *Streptococcus pyogenes*

Received for publication, October 24, 2023, and in revised form, December 4, 2023 Published, Papers in Press, January 3, 2024,
https://doi.org/10.1016/j.jbc.2023.105623

Emma-Jayne Proctor[1], Hannah R. Frost[2], Sandeep Satapathy[1,3], Gwenaëlle Botquin[2], Joanna Urbaniec[1], Jody Gorman[1], David M. P. De Oliveira[4], Jason McArthur[1], Mark R. Davies[5], Anne Botteaux[2], Pierre Smeesters[2], and Martina Sanderson-Smith[1,*]

From the [1]Molecular Horizons and School of Chemistry and Molecular Bioscience, University of Wollongong, Wollongong, Australia; [2]Molecular Bacteriology Laboratory, European Plotkins Institute for Vaccinology (EPIV), Université Libre de Bruxelles, Brussels, Belgium; [3]The Broad Institute of MIT and Harvard, Cambridge, Massachusetts, USA; [4]The University of Queensland, School of Chemistry and Molecular Biosciences, Australian Infectious Diseases Research Centre, QLD, Australia; [5]Department of Microbiology and Immunology, at the Peter Doherty Institute for Infection and Immunity, The University of Melbourne, Victoria, Australia

Reviewed by members of the JBC Editorial Board. Edited by Chris Whitfield

Group A Streptococcal M-related proteins (Mrps) are dimeric α-helical-coiled-coil cell membrane-bound surface proteins. During infection, Mrp recruit the fragment crystallizable region of human immunoglobulin G *via* their A-repeat regions to the bacterial surface, conferring upon the bacteria enhanced phagocytosis resistance and augmented growth in human blood. However, Mrps show a high degree of sequence diversity, and it is currently not known whether this diversity affects the Mrp–IgG interaction. Herein, we report that diverse Mrps all bind human IgG subclasses with nanomolar affinity, with differences in affinity which ranged from 3.7 to 11.1 nM for mixed IgG. Using surface plasmon resonance, we confirmed Mrps display preferential IgG-subclass binding. All Mrps were found to have a significantly weaker affinity for IgG3 ($p < 0.05$) compared to all other IgG subclasses. Furthermore, plasma pulldown assays analyzed *via* Western blotting revealed that all Mrp were able to bind IgG in the presence of other serum proteins at both 25 °C and 37 °C. Finally, we report that dimeric Mrps bind to IgG with a 1:1 stoichiometry, enhancing our understanding of this important host–pathogen interaction.

Streptococcus pyogenes (Group A *Streptococcus*; GAS) is a Gram-positive, exclusively human pathogen responsible for a range of clinical manifestations encompassing self-limiting superficial infections, to severe invasive diseases and post-infection sequelae. These conditions are estimated to cause over 18 million infections and >500,000 deaths per year (1, 2). The M protein family are major GAS virulence factors expressed on the bacterial surface and consist of the M protein (M), M-related protein (Mrp), and M-like Protein (Enn) (3). These proteins are colocated within the multiple gene activator (*mga*) regulon and encoded by the *emm*, *mrp*, and *enn* genes, respectively, and their presence is variable in the global population (3, 4). The M protein family has been reported to contribute to GAS virulence through binding of several plasma proteins (5, 6).

Accounting for 10 to 20% of protein in human serum, the highly abundant immunoglobulin G (IgG) is essential in the immune response to pathogens (7). While all IgG share 90% amino acid sequence homology, IgG can be divided into four subclasses with varying abundance in serum and roles in the immune response (7). For example, IgG1 is the most abundant IgG subclass, responsible for eliciting an antigen-specific immune response to soluble protein antigens and membrane proteins (8). For bacterial capsular polysaccharide antigens, IgG2 is the principal response (9). IgG3-dominated responses are generally limited to viral infections (10), whereas IgG4-directed responses are induced by allergens, resultant of long-term exposure to antigens from a noninfectious settings (11). Preferential IgG subclass responses are commonly observed as a reaction to different antigens, resulting in the activation of different components of the immune response (7). This can be observed in pathologies as, for example, deficiencies in IgG2 responses have been associated with increased susceptibilities to bacterial infection (9).

The Mrp has been identified as a GAS IgG-binding protein, with the interaction occurring between the N-terminal A-repeat region of Mrp and the Fc-region of human IgG, a mechanism of immune evasion by the bacteria known as nonimmune binding (12). The interaction between these respective protein families is facilitated by the dimeric α-helical coiled-coil conformation of the Mrp, also observed in Enn and M proteins (13–18). Within a single Mrp molecule, the presence of A-repeat sequences on each monomer within the native dimer allows for the existence of two potential IgG-binding sites. However, the stoichiometry of Mrp-IgG is yet to be experimentally defined (16). Mrp-mediated recruitment of IgG by GAS has been shown to assist phagocytosis resistance and enhance growth of GAS in human blood (12, 19–21). Given that Mrp is present within 88.9% of all GAS

* For correspondence: Martina Sanderson-Smith, martina@uow.edu.au.

isolates and all Mrp to date contain the A-repeat region, it has been suggested IgG binding is a conserved function of all Mrp (4, 22). A recent study examining the Mrp amino acid sequences from a global collection of 1668 GAS genomes revealed an average pairwise identity of 83.2% (4). The impact of this diversity on the interaction between Mrp and IgG has not been investigated, and the IgG-binding site within Mrp has only been characterized for one Mrp variant (Mrp4), derived from a single GAS isolate (12). Deletion of Mrp4 was reported to result in a 70% reduction in IgG binding to GAS in human blood compared to wildtype (12). However, it is unclear if IgG binding is conserved among diverse Mrp. Furthermore, while preferential subclass binding has been observed for Mrp4 in the order of IgG1>IgG4>IgG2>IgG3 for a single strain of GAS (12), it is unclear whether variations in Mrp sequence influence preferential IgG-subclass binding.

Herein, nine representative Mrp sequences from a global diverse GAS database were chosen for analysis. In this study, we evaluate the affinity of distinct Mrp for various IgG subtypes and determine if diverse Mrp preserve the ability to bind IgG in human plasma. Using Mrp216, a protein with significant homology to ∼60% of Mrp, we report the binding stoichiometry and subclass preferences of Mrp. *In vitro* characterization concluded that Mrp with various amino acid sequences maintained binding to all IgG subclasses with nanomolar affinity. Furthermore, in the presence of other serum proteins, the Mrp–IgG interaction was retained, and the interaction between dimeric Mrp and IgG was found to exist at a 1:1 stoichiometry. Mrp also showed preferential subclass binding to IgG1, IgG2, and IgG4 and a statistically significantly lower affinity for IgG3. Taken together, these data demonstrate that the Mrp–IgG interaction is conserved among structurally diverse Mrp, suggesting that the Mrp–IgG interaction is an important host–pathogen interaction in GAS virulence.

Results

Mrp selection

The global diversity of Mrp has been evaluated, from a database of 1688 GAS genomes (4, 23) and characterized into four genetically distinct groups (24). Within these four groups, nine representative Mrps were selected, based on genetic variability, to investigate the effect of Mrp diversity on binding to human IgG (Table 1 and Fig. 1). The amino acid pairwise identity between Mrp in this study ranges from 74.9 to 99.1% (Fig. 1). The nine Mrp were derived from GAS strains of various clinical origins (25), exhibiting extensive *emm* and *enn* type diversity, associated with an array of *emm* and *enn* clusters (26). The amino acid coordinates of the mature Mrp used in functional studies and the Mrp ORF are reported in Table 1.

The IgG-binding sequence of Mrp is conserved among genetically diverse Mrp

The IgG-binding sequence is located within the A-repeat region of Mrp, downstream the hypervariable N-terminal domain (12). To compare the IgG-binding motif in the Mrp in this study, a pairwise MUSCLE alignment of the A-repeat region (Fig. 2*A*) and the amino acid frequency at each position was assessed (Fig. 2*B*). This analysis confirmed that all Mrp in this study have three A-repeat sequences (Fig. 2*B*), each with an average pairwise identity of >94%, much higher than the sequence identity of full-length proteins (Fig. 1), suggesting that the IgG-binding sequence of Mrp is highly conserved (Fig. 2*A*).

Mrp secondary structure

The α-helical-coiled-coil conformation has been described as essential for the interaction of M and M-like proteins with several plasma proteins (13–16). The probability of an α-helical coiled-coil conformation was assessed for the nine Mrp using ExPASy Coils (Fig. 3*A*). Variation in the prediction of α-helical coiled-coil structure between Mrp for the N-terminal variable region (aa 49–90) supports previous research demonstrating that the structural diversity of Mrp arises in this region. An α-helical coiled-coil structure was predicted for the IgG-binding A-repeats as well as the remainder of the extracellular portion of all nine Mrp (aa 180–220). Far UV circular dichroism (CD) spectroscopy confirmed all Mrp in this study exhibited minima at 222 nm and 208 nm and a maximum peak at 190 nm (Fig. 3*B*). Furthermore, for all Mrp the 222:208 nm ratio was greater than ∼1 (Table S2). These data are characteristic of α-helical coiled-coil protein (27). Using BeStSel software (28), the Far-UV CD spectra were deconvoluted to

Table 1
Details of the GAS strains from which the Mrp examined in this study were derived

Strain name	Strain origin	*mrp* type[a]	*Mrp* Primary groups[a]	Mrp ORF (bp)	Amino acid coordinates Of mature Mrp used in functional studies	*emm* type[b]	*emm* cluster[b]	*enn* type[a]	Ref.
939–03	Skin sore	298	1	1257	1–343	117.1	E2	120	(23)
NS931	Necrotizing fasciitis, blood	8	2	1275	1–349	69	E6	183.2	(55)
PRS66	Origin unknown	52	2	1275	1–348	102	E4	152	(24)
NS192	Renal transplant, septic (blood)	71	3	1245	1–339	106	E2	155.1	(55)
NS210	Diabetic ulcer with fever	105	3	1245	1–339	22	E4	342	(55)
NS80	Blood	193	4	1164	1–311	70	D4	233	(56)
NS88.2	Blood	216	4	1164	1–312	98	D4	315	(55)
NS730	Necrotizing fasciitis, pus from left hip	115	4	1152	1–307	90	E2	3	(55)
NS452	Cellulitis, wound	174	4	1152	1–308	25	E3	83	(55)

[a] The *mrp* and *enn* type and *mrp* grouping were as per (24).
[b] The *emm* type and cluster assignments were as per (25).

	Mrp298	Mrp8	Mrp52	Mrp71	Mrp105	Mrp193	Mrp216	Mrp115	Mrp174
Mrp298		75.7%	75.4%	75.9%	75.5%	80.6%	79.7%	81.5%	83.2%
Mrp8	75.7%		92.7%	81.6%	81.8%	81.8%	81.1%	82.6%	84.1%
Mrp52	75.4%	92.7%		80.5%	81.8%	83.3%	82.5%	83.1%	84.6%
Mrp71	74.9%	81.6%	80.5%		92.0%	80.5%	79.6%	81.1%	82.6%
Mrp105	75.5%	81.8%	81.8%	92.0%		81.6%	80.7%	81.7%	83.1%
Mrp193	80.6%	81.9%	83.3%	80.5%	81.6%		99.1	95.1%	95.6%
Mrp216	79.7%	81.1%	82.5%	79.6%	80.7%	99.1		94.2%	94.8%
Mrp115	81.5%	82.6%	83.1%	81.1%	81.7%	95.1%	94.2%		97.4%
Mrp174	83.2%	84.1%	84.6%	82.6%	83.1%	95.6%	94.8%	97.4%	

Figure 1. Pairwise amino acid sequence identity for nine globally representative Mrp sequences. Pairwise MUSCLE alignment using default settings in Geneious (version 6.0, Biomatters) defined the percentage sequence identity between the nine Mrp in this study at the amino acid sequence level. Prior to the analysis, the signal peptide at the N terminus and the region encoding and downstream the LPXTG motif at the C terminus were removed to reveal the mature Mrp sequence for evaluation. The percentage of residues that are identical between the Mrp sequences (% identity) is presented as a heat map whereby *darker shades* correspond to increased % identity between Mrp. Mrp, M-related protein.

obtain predictions of the relative abundance of different secondary structures in Mrp, including α-helix, β-strand, and turns (Table S2). These data revealed α-helices as the predominant secondary structure in all Mrp. Mrp216 and Mrp193 exhibited 57.9% and 56.5% α-helix, respectively, while Mrp105 and Mrp71 were 82.3% and 78.3% α-helix. All other Mrp examined were suggested to contain >92.8% α-helix.

Mrp binds IgG with high affinity

Functional characterization of IgG binding to the whole Mrp was carried out to determine any differences in IgG-binding capacity (Figs. 4 and S1). Surface plasmon resonance (SPR) was utilized to confirm and compare the interaction between the various Mrp and IgG. All Mrp demonstrated a concentration-dependent increase in IgG binding, exemplified

A

	Mrp298	Mrp8	Mrp52	Mrp71	Mrp105	Mrp193	Mrp216	Mrp115	Mrp174
Mrp298		99.0%	98.1%	98.1%	97.1%	97.1%	95.2%	97.1%	98.1%
Mrp8	99.0%		99.0%	97.1%	98.1%	98.1%	96.2%	98.1%	99.0%
Mrp52	98.1%	99.0%		96.2%	99.0%	99.0%	97.1%	97.1%	98.1%
Mrp71	98.1%	97.1%	96.2%		95.2%	95.2%	93.3%	95.2%	96.2%
Mrp105	97.1%	98.1%	99.0%	95.2%		98.1%	96.2%	96.2%	97.1%
Mrp193	97.1%	98.1%	99.0%	95.2%	98.1%		98.1%	98.1%	99.0%
Mrp216	95.2%	96.2%	97.1%	93.3%	96.2%	98.1%		96.2%	97.1%
Mrp115	97.1%	98.1%	97.1%	95.2%	96.2%	98.1%	96.2%		99.0%
Mrp174	98.1%	99.0%	98.1%	96.2%	97.1%	99.0%	97.1%	99.0%	

B

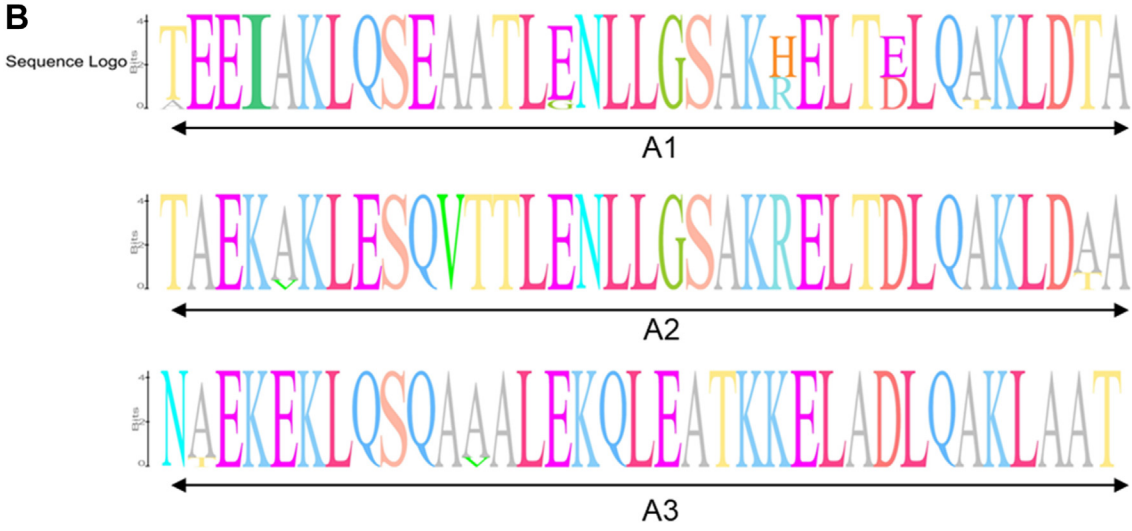

Figure 2. Comparison of IgG-binding sequences in nine diverse Mrp. (*A*), a pairwise identity analysis was produced to reveal the percentage of residues that are identical between the Mrp sequences in this study within the A-repeat region. The pairwise MUSCLE alignment tool was used under default settings in Geneious (version 6.0, Biomatters), and the pairwise identity was visualized a heat map. *Darker shades* correspond to increased % identity between Mrp. (*B*), the amino acid frequency at the IgG-binding domain (A-repeat region) is shown as a graphical representation for the nine representative proteins used in this study. Mrp, M-related protein; IgG, immunoglobulin G.

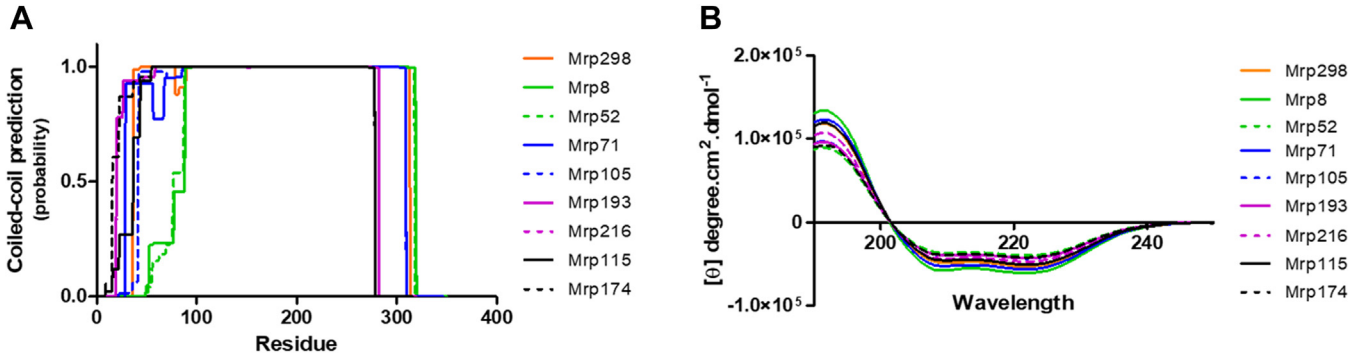

Figure 3. Comparison of secondary structure of nine diverse Mrp. (*A*), probability of Mrp to adopt a coiled-coil secondary structure. Amino acid sequences were analyzed in ExPASy Coils. (*B*), circular dichroism spectra of genetically distinct recombinant Mrp. All Mrps have CD absorption spectra indicative of α-helical coiled-coil proteins, as there are two minima at approximately 210 nm and 220 nm and a maximum peak at 190 nm. Mrp, M-related protein.

by the sensogram for the interaction between Mrp216 and IgG (Fig. 4*A*). The nonlinear fitting of all sensograms according to a 1:1 Langmuir binding model (Fig. 4*B*) allowed for the calculation of the steady-state affinity constant (equilibrium dissociation constant; K_D) (Table 2). Scatchard plot analysis (Fig. 4*C*) yielded a linear plot for Mrp and IgG typical of a monovalent interaction (Fig. 4*C*). Comparison of the obtained K_D values confirmed that that all groups of Mrp can bind human IgG with nanomolar affinity (Table 2).

1:1 stoichiometric interaction between dimeric Mrp216 and IgG

M and Mrp have been shown to exist in a dimeric state which, for M proteins, is stabilized in the presence of several host ligands including IgG (13, 16–18). Scatchard plot analysis of SPR data suggested a 1:1 stoichiometry between Mrp and IgG, so, to further assess the stoichiometry of the interaction between Mrp and IgG, mass photometry was used to determine the relative distribution of monomeric and oligomeric forms of Mrp216, which shares significant genetic homology with approximately 60% of Mrp (Fig. 5) (26). Mrp216 was found to exist as a dimer (70 kDa) (Fig. 5*B*), and human IgG was present at the molecular weight of monomeric IgG at 150 kDa (Fig. 5*A*). Analysis of Mrp216: IgG complexes revealed the presence of a single species with a molecular mass of 220 kDa at both 1:1, 10:1, and 1:10 Mrp:IgG molar ratios (Fig. 5, *E H*, and *K*). This corresponds to the expected size of a complex formed *via* a 1:1 stoichiometric interaction between dimeric Mrp216 and IgG.

The dimeric M proteins M1 and M54 were also used as positive and negative IgG-binding controls, respectively. Analysis of the IgG binding M1 protein (Fig. 5*C*) confirmed the expected molecular weight of the dimeric M protein (80 kDa), while the non-IgG binding M54 protein predominately existed as a dimer (85 kDa) with some protein present as a tetramer (174 kDa) (Fig. 5*D*). Mass photometry analysis of M1: IgG complexes revealed the presence of a single species with a molecular mass of 232 kDa when examined at 1:1 (Fig. 5*F*) M1:IgG molar ratios. This corresponds to the expected size of a complex formed *via* a 1:1 stoichiometric interaction between dimeric M1 and IgG. At a ratio of 1:10 (Fig. 5*I*) M1:IgG, the 1:1 stoichiometric complex is present along with an abundance of excess IgG, suggesting saturation of IgG-binding sites on Mrp at the 1:1 stoichiometric ratio. At a molar ratio of 10:1 (Fig. 5*L*) M1:IgG, multiple binding stoichiometries are present in solution, with the 1:1 complex as the predominant species. An additional species is present at a mass of 303 kDa that may indicate two dimers of M1 and a single IgG, a stoichiometry previously reported by Khakzad *et al*. (29), although an alternative explanation for this species may be that it represents an IgG dimer. A minor species constituting 3% of all proteins detected is also reported at 390 kDa that may represent two IgG interacting with one

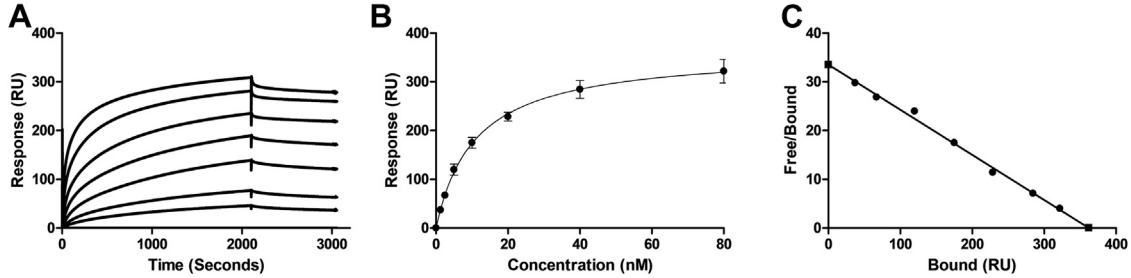

Figure 4. SPR analysis of the interaction between human IgG and Mrp. (*A*), representative SPR sensogram generated using steady-state mode for the interaction between Mrp216 and IgG. All assays were performed using IgG in a concentration series of 0 to 80 nM over a succession of seven separate injections for 2100s at a flow rate of 10 μl/min followed by a 900s dissociation period. (*B*), the steady-state affinity analysis was produced by the nonlinear fitting of sensorgrams according to a 1:1 Langmuir binding model in BIAevaluation, *version* 4.0.1 (Biacore AB). IgG, immunoglobulin G; Mrp, M-related protein; SPR, surface plasmon resonance.

Table 2
Comparison of steady-state affinity (K_D) for genetically diverse Mrp (nM)

mrp type	IgG[a]	IgG1	IgG2	IgG3	IgG4
298	9.3 ± 2.8	16.0 ± 1.5	19.4 ± 1.4	226.0 ± 12.9	13.4 ± 2.0
8	8.3 ± 0.7	15.3 ± 2.2	21.8 ± 2.9	255.6 ± 10.7	11.9 ± 2.3
52	3.9 ± 0.3	3.0 ± 0.7	6.4 ± 2.4	144.6 ± 6.8	9.02 ± 1.2
71	11.1 ± 1.7	11.1 ± 0.5	15.4 ± 1.9	219.6 ± 24.7	15.2 ± 0.8
105	3.7 ± 0.2	7.0 ± 0.4	7.03 ± 0.3	207.7 ± 4.6	10.6 ± 0.5
193	6.4 ± 1.7	5.0 ± 0.2	8.17 ± 1.0	201.0 ± 6.8	6.5 ± 0.7
216	5.0 ± 0.2	5.4 ± 0.6	8.12 ± 1.4	301.6 ± 28.2	4.3 ± 0.6
115	10.2 ± 1.1	13.4 ± 1.7	13.54 ± 2.0	244.0 ± 8.2	7.4 ± 1.8
174	8.8 ± 1.3	9.71 ± 0.7	11.03 ± 0.4	151.6 ± 6.5	11.9 ± 0.8

Data represent the mean ± SEM in nM as determined from three experimental replicates.
[a] This IgG fraction contains pooled mixture of all IgG subclasses found in serum.

dimer of M1. Conversely, there was no evidence of complex formation between the negative control proteins M54 and IgG at both 1:1 (Fig. 5*G* and 1:10 (Fig. 5*J*) M:IgG molar ratios, with mass photometry revealing the presence of two species corresponding to the molecular size of IgG (150 kDa) and dimeric M54 (87 kDa).

IgG binding is retained in the complex plasma-binding environment

Mrp has been shown to interact with other host proteins in plasma (5) and therefore the ability of Mrp to bind IgG may be altered in this complex host environment. To demonstrate the availability of the IgG-binding domain of Mrp in a physiologically complex environment, plasma pulldown assays were performed (Fig. 6). Analysis of all the elution fractions from the pulldown assays confirmed the co-elution of Mrp and IgG for all nine Mrp at both at 25 °C (Fig. 6*A*) and 37 °sC (Fig. 6*B*).

Mrp demonstrates preferential IgG subclass binding

The identification of Mrp subclass preferences may provide insight into mechanisms of GAS virulence, as skewed subclass preferences can alter the host immune system response (7). To determine if subclass preferences is conserved for genetically diverse Mrp, SPR experiments conducted in steady-state mode were conducted to confirm and compare the strength of the interaction for the nine representative recombinant Mrp to each IgG-subclass (Figs. S2–S5). All nine Mrp could bind all IgG subclasses, and preferential IgG subclass binding was identified for all Mrp by the steady-state affinity plots generated from the nonlinear fitting of the sensogram's according to a 1:1 Langmuir binding model to determine the K_D (Table 2). The steady-state affinity plots for Mrp216 and IgG1 (Fig. 7*A*), IgG2 (Fig. 7*B*), and IgG4 (Fig. 7*D*) revealed that 40 nM of IgG1, IgG2, and IgG4 was required to reach plateau. Conversely, IgG3 did not reach plateau even at concentrations as high as 800 nM IgG (Fig. 7*C*). A two-way ANOVA and Bonferroni post-test analysis of the K_D of all nine Mrp to IgG1, IgG2, IgG3, and IgG4 confirmed no significant difference in binding affinity for Mrp to IgG1, IgG2, and IgG4 ($p > 0.05$) (Table 2). All nine Mrp in this study demonstrated a significantly lower affinity for IgG3 ($p \leq 0.001$) (Table 2).

Discussion

The binding of human IgG by an Mrp has been shown previously to enhance GAS growth and phagocytosis resistance during infection (12, 19–21). Recently, the genetic diversity of Mrp within a global GAS population was defined (4), raising questions as to the functional diversity of different Mrp. Here, our study aimed to better elucidate the mechanism of interaction between Mrp and IgG. We report that diverse Mrp (1) bind human IgG with nanomolar affinity; (2) bind IgG1, IgG2, and IgG4 subclasses with comparable affinity yet have significantly reduced affinity for IgG3; and (3) retain IgG-binding capacity in plasma. Further, we report for the first time that dimeric Mrp binds IgG in a 1:1 complex.

Despite amino acid pairwise sequence diversity as low as 75%, all nine Mrp characterized in this study displayed CD spectra representative of α-helical proteins, in support of previous findings (16). This is the first study to report that Mrp bind IgG with nanomolar affinity. Previous work has shown that GAS express several high-affinity IgG-binding proteins, including M1, M22, and Protein H (Sph), that bind IgG with a K_D affinity constant in the range of 0.4 nM to 10 μM affinity (13, 25, 30–33). The proposed IgG-binding domain within the Mrp is similar to the known fragment crystallizable region of human IgG-binding region of the M1 protein (12, 34). The M1 protein binds IgG *via* a 38 amino acid sequence called the S-region, located at the end of the variable region before the C-repeat domain of the protein (35). This S-region has 42% identity and 66% similarity to the Mrp A-repeat region (36). Protein H binds to IgG *via* a bipartite sequence, including a 28 amino acid sequence called G1234, which is followed by a 35 amino acid EQ-rich region composed of greater than 50% Gln and Glu (37). The M1 protein and Sph are associated with GAS strains which lack Mrp, confirming conservation of IgG binding amongst GAS isolates, despite genetic differences between strains (25, 38, 39). The existence of multiple mechanisms of IgG binding amongst GAS strains highlights the potential importance of IgG binding to GAS virulence. Additionally, studies have shown differences in the presence and orientation of IgG at the surface of GAS isolated from different sites of infection (40). Therefore, understanding the mechanism of IgG recruitment by GAS may provide insight into the molecular mechanisms underlying the severity of infection.

Previous reports indicate that M and Mrp exist in a dimeric state which can affect interactions with various host ligands,

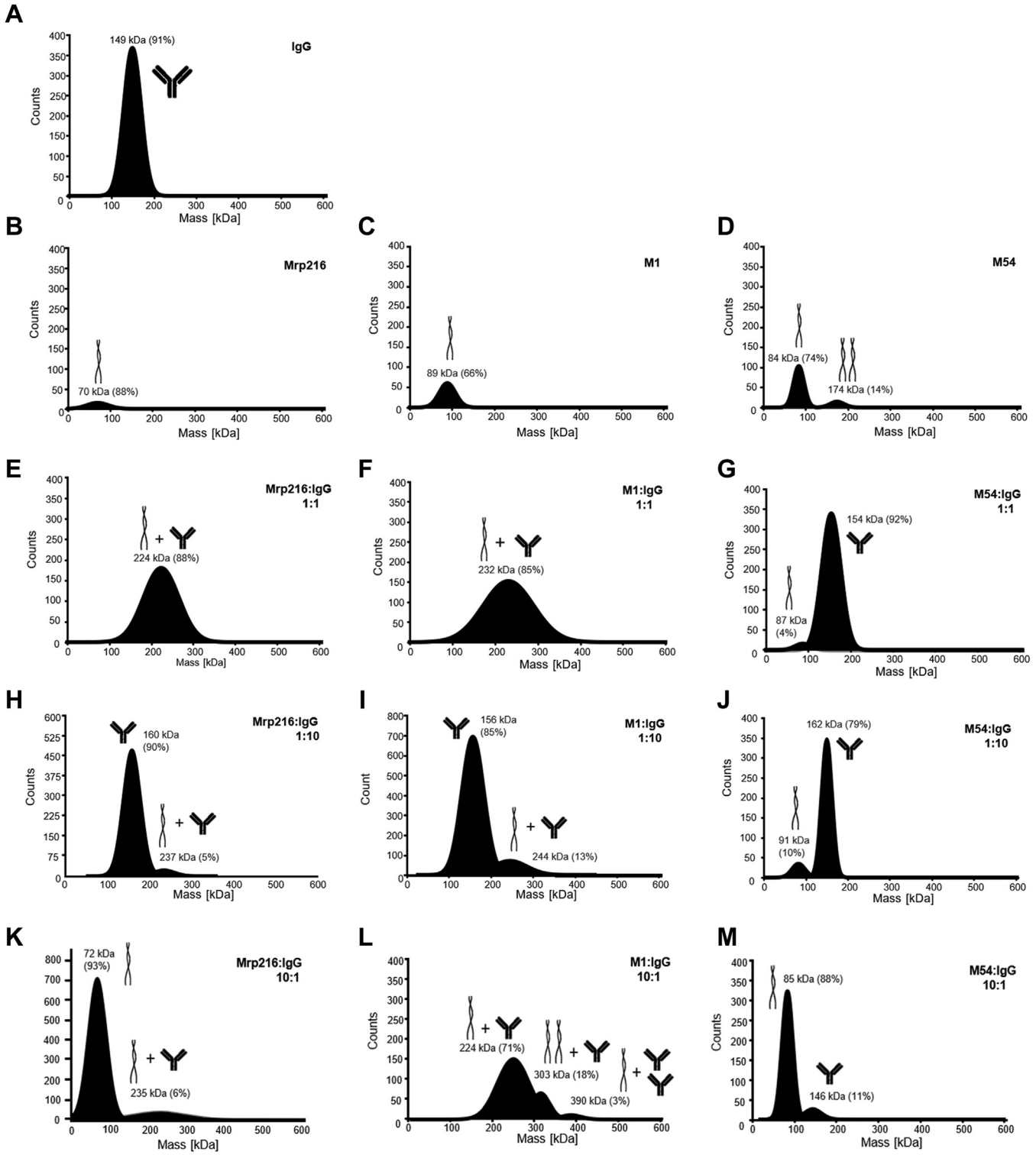

Figure 5. Determination of binding stoichiometry for Mrp216 and IgG using mass photometry. (*A*) human IgG was analyzed as a control, (*B*) Mrp216, (*C*) M1 protein (IgG-binding positive control), and (*D*) M54 protein (IgG-binding negative control) were analyzed individually, each at a concentration of 100 nM. *E–G*, analysis of (*E*) 1:1 Mrp216: IgG and (*F*) 1:1 M1: IgG demonstrates a MP mass distribution shift that is not evident in (*G*) 1:1 M54: IgG. Analysis of (*H*) 1:10 Mrp216: IgG and (*I*) 1:10 M1: IgG demonstrates a MP mass distribution shift that is not evident in (*J*) 1:10 M54: IgG. *K–M*, analysis of (*K*) 10:1 Mrp216: IgG and (*L*) 10:1 M1: IgG demonstrates a MP mass distribution shift that is not evident in (*M*) 10:1 M54: IgG. The percentage indicated on each peak for all graphs indicates the number of events detected. Data are representative of two independent experiments. IgG, immunoglobulin G; Mrp, M-related protein.

for example the dimerization of M1 was shown to be required for IgG binding (13, 16–18). M1 dimerization was found to be temperature dependent, with M1 protein predominantly existing as a monomer at 37 °C, the physiological temperature in deep tissue and blood infections (33). M1 exists as a dimer at 25 °C, a temperature encountered by GAS in peripheral

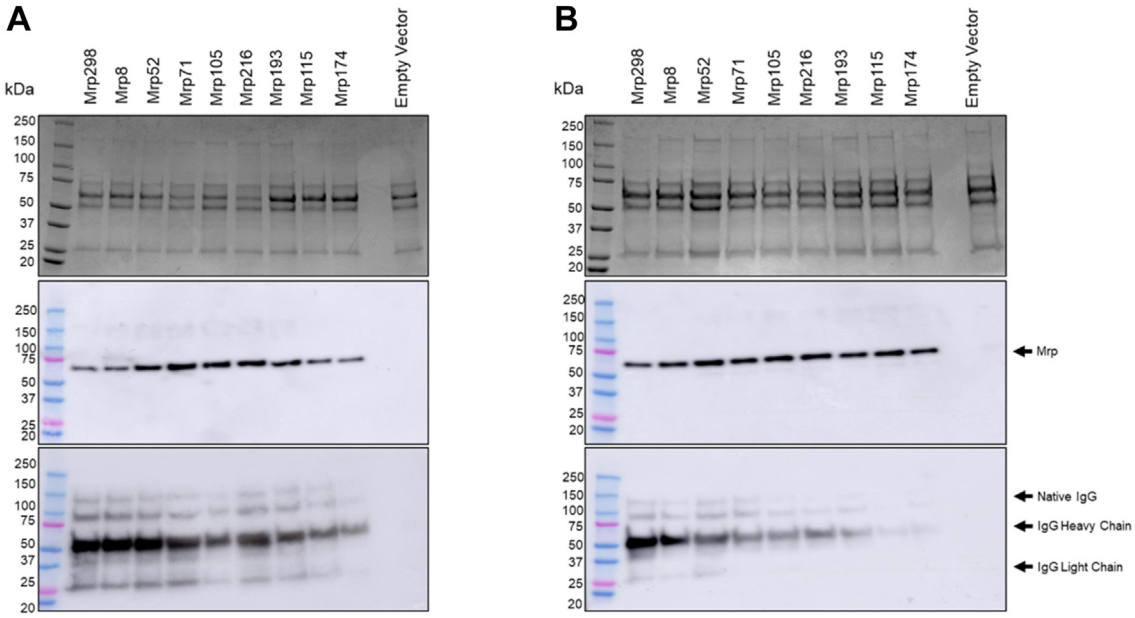

Figure 6. Interaction between Mrp and IgG detected in human plasma. *A* and *B*, plasma pulldown assays were performed using NiNTA affinity chromatography on the lysates of BL21/DE3 *E.coli* expressing the nine 6x His-tagged Mrp at (*A*) 25 °C and (*B*) 37 °C to assess the acquisition of IgG by Mrp. 4 to 20% Mini-PROTEAN TGX Stain-Free SDS-PAGE gels (Bio-Rad) were loaded with 8ug of total protein from the pooled elution fractions, and IgG was detected by immunoblotting onto PVDF membranes (Bio-Rad). Total protein in each elution fractions is shown in the upper panel *via* Coomassie blue staining. The middle panel confirmed the presence of all Mrp using a mouse anti-6x His-tag antibody 27E8 (#2336, Cell Signaling Technology). The *lower panel* demonstrates the presence of IgG *via* detection with a goat anti-human (H + L HRP conjugate (#1721050, Bio-Rad). As a control, the experiment was conducted in lysates of BL21/DE3 *E. coli* cells transformed with pGEX4T1 alone, without Mrp (vector only), and no Mrp or IgG was detected in these samples. IgG, immunoglobulin G; Mrp, M-related protein.

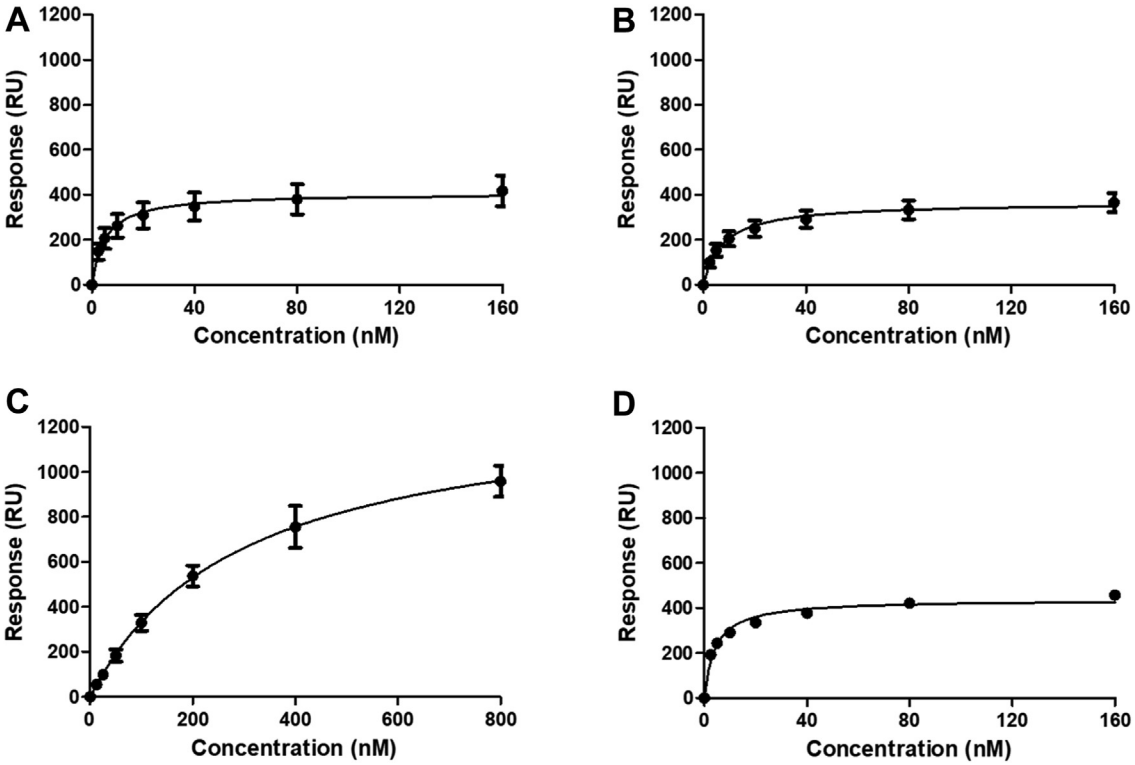

Figure 7. Binding of IgG subclasses to the M-related protein. *A–D*, steady-state affinity plot for the interaction between Mrp216 and (*A*) IgG1, (*B*) IgG2, (*C*) IgG3, and (*D*) IgG4. The concentration range of 0 to 800 nM of IgG was examined during SPR experiments in steady state mode. Each analyte concentration was examined independently, with an injection time of 2100s at a flow rate of 10 µl/min followed by a 900s dissociation period. The steady-state affinity plots were produced by the nonlinear fitting of sensorgrams according to a 1:1 Langmuir binding model in BIAevaluation, *version* 4.0.1 (Biacore AB). IgG, immunoglobulin G; SPR, surface plasmon resonance.

tissues during superficial pharyngeal and skin infections (17, 33). The physiological consequences of temperature dependent binding of M proteins to host proteins was suggested to alter the host–pathogen relationship during infection, by potentially allowing the pathogen to modify its surface properties in different environments (33). Here, we confirm that both Mrp, like M proteins, exist predominately in the dimeric state *in vitro* at 25 °C. The thermal stability of Mrp has previously been investigated, and Mrp4 was shown to exist as a thermally stable coiled-coil dimer up to temperatures of 70 to 90 °C and maintained ligand binding to fibrinogen, another serum protein (16). Here, we have shown that there is structural diversity between different Mrp at 25 °C, highlighting the need for future studies to consider the role of thermal stability of the Mrp family in ligand binding.

Previous reports suggest up to two dimeric M1 proteins may interact with a single Ig gG-Fc *via* the M1 S-region/C1-domain using cross-linking mass spectrometry and molecular dynamics simulations (29), and mass photometry data presented here further support this stoichiometry for M1–IgG interactions. However, Mrp were only found to interact with IgG at a 1:1 stoichiometric ratio, even when either protein was provided in a 10-fold molar excess. Sequence homology between the M1 S-region/C1-domain and the Mrp A-repeat region is approximately 42% (36), therefore sequence differences between this IgG-binding domain of M1 and Mrp may explain differences in binding stoichiometries. Alternatively, binding of Mrp to IgG *via* the A-repeat may be conformationally driven such that the dimeric structure of Mrp is required to elicit IgG binding.

Moreover, we have shown that dimeric M1 displays multiple binding stoichiometries with IgG. Complexes corresponding to a single M1 and two IgG molecules were also detected in the current study. This supports previous reports of a secondary IgG-binding site on IgG in the A-repeat region of M1 (29), whereby IgG may be capable of binding at the two independent binding sites on M1 (S-region/C1-domain and the A-repeat region). However, this 1:2 M1:IgG species was rare, representing only 3% of the total population of complexes detected in experiments. It should be noted that Khakzad *et al.* (29) assessed the interaction with M1 and IgG following incubation of whole bacteria in human plasma. The differences in stoichiometry between our study and this previous work may reflect differences between M1 in its soluble form and when bound to the GAS cell surface. During invasive infections, M proteins can be cleaved from the cell surface to exist in a soluble form *via* the bacterial secreted cysteine protease (SpeB) and neutrophil proteases (41, 42).

GAS likely encounters host IgG in a complex environment where other host proteins are abundant (43). We sought to determine if the ability of Mrp to bind IgG may be altered in this complex host environment. Mrp has previously been shown to interact with fibrinogen, via two domains in the N-terminal region of Mrp (22). The fibrinogen and IgG-binding domains are separate and distinct, and Mrp retains its fibrinogen binding capacity upon deletion of the A-repeat domain (12). Other than fibrinogen, no other Mrp-binding partners have been characterized from human plasma. Further analysis is required to determine if other plasma proteins commonly acquired by GAS during infection are capable of binding Mrp (25). All nine Mrp bound IgG in human plasma, suggesting the Mrp contains a highly specific IgG-binding site that is accessible in the presence of other Mrp ligands.

Our finding that Mrp have a significantly lower affinity for IgG3 are in accordance with previously published findings using alternative experimental methods including competitive inhibition assays and Ouchterlony immunodiffusion (12, 20, 44). However, previous reports suggest that some M family proteins do not interact with IgG3 at all (45, 46). Our data suggest that the interaction of the M-family of proteins with IgG3 is weak, and it is possible that the weak interaction between Mrp and IgG3 was not observed in previous studies due to methodologies with lower sensitivity. IgG3 has a mean adult serum level of 0.51 g/L and has a relative abundance of 5 to 8% of total serum IgG (7). Therefore, since the abundance of IgG3 is low and elicited primarily in response to viral infection, reduced binding of Mrp to IgG3 may be because GAS has adapted to recognize more abundant subclasses to maximize IgG binding. While all IgG subclasses share 90% homology, IgG3 has a much longer hinge region than other subclasses (47). This gives IgG3 a greater flexibility, which is said to contribute to IgG3's enhanced effector functions. These effector functions are mediated by the Fc region of IgG, which can activate the classical complement pathway through its interaction with C1q and binding Fcγ receptors on immune cells that trigger phagocytosis, reactive oxygen species production, and other immune effectors (48, 49). The structural differences between IgG3 and all other subclasses may give rise to the reduced binding of Mrp to IgG3. However, the Enn proteins from the 64/14, M18, and M5 GAS strains are also able to bind IgG3 (34, 50). Thus, for these isolates, IgG3 binding is likely conserved despite the reduced affinity of Mrp for IgG (4, 25).

Mrp is present in 64.4% of *emm* types responsible for global infections suggesting that Mrp plays a significant role in GAS virulence (4). Mrp has recently been included in a 30-valent vaccine candidate to broaden vaccine coverage; however, our understanding of the role of Mrp in GAS virulence is still limited, in comparison to other vaccine antigens (51). Here, we demonstrate that diverse Mrp bind IgG with high affinity and specificity, with preferential recognition of IgG subclasses 1, 2, and 4. Furthermore, we show for the first time that Mrp binds IgG in with 1:1 stoichiometric ratio, providing new insight into the mechanisms of Mrp IgG interaction (4).

Experimental procedures

Ethics statement

All experiments involving the use of human plasma were conducted with informed consent of healthy volunteers, approved, and authorized by the University of Wollongong Human Research Ethics Committee (Protocol HE08/250) and abide by the Declaration of Helsinki Principles.

Bioinformatics analysis of Mrp primary and secondary structure

Nine Mrp representing the global genetic diversity of Mrp were chosen from a previous genetic analysis to represent the four groups and nine subgroups (24). The locus tags for each Mrp are presented in Supporting Information Table S1. A pairwise identity analysis was generated for the nine Mrp in this study *via* the pairwise MUSCLE alignment tool using default settings in Geneious, *version* 6.0 (Biomatters). The amino acid portion representing the signal peptide at the N terminus and the C-terminal region encoding the cell wall anchoring LP*X*TG motif was removed from the Mrp sequence prior to the alignment. A distance matrices of amino acid identities were generated for full mature Mrp protein sequences and each A repeat sequence in Geneious, *version* 6.0 (Biomatters). The probability of Mrp to adopt a coiled-coil secondary structure was assessed for the nine Mrp using ExPASy Coils (Swiss Institute of Bioinformatics) as previously described (52) and plotted in GraphPad Prism, *version* 5 (GraphPad Software).

Bacterial strains, culture conditions

E. coli BL21/DE3 (Invitrogen) strains containing expression plasmids were cultured aerobically on Luria Bertani (LB) agar supplemented with 100 μg/ml ampicillin (Ap100) (Astral Scientific) at 37 °C for 16 h. Liquid cultures were grown at 37 °C overnight with agitation (150 rpm) in LB broth supplemented with Ap100 (53). GAS strains (Table 1) were routinely cultured at 37 °C on horse-blood agar (Oxoid) for 16 h. Liquid GAS cultures were grown at 37 °C overnight in Todd-Hewitt broth (Bacto Laboratories) supplemented with 1% yeast extract (Sigma) (THY).

DNA manipulations and cloning constructs

Nine Mrp genes, excluding the N-terminal signal peptide and C-terminal cell wall anchoring domain, were used for functional analyses (Table 1). Additionally, a C-terminal hexahistidyl tag (6x His-tag) and stop codon (TAA) was incorporated into each sequence. The recombinant Mrp gene was subcloned into pGEX4T1 (Invitrogen) by Genscript *via* the *Bam*HI and *Eco*RI restriction enzyme sites, resulting in an N-terminal fusion with glutathione S-transferase (GST). The presence of both a 6x His-tag and a GST tag on the recombinant protein enabled purification. The positioning of the C-terminal 6x His-tag also ensures that Mrp is captured and presented in a homogenous orientation on the sensor surface in SPR experiments providing a physiologically relevant comparison of each binding interaction as MRP is anchored into the GAS cell surface *via* the C-terminal portion with the N-terminal portion extending distally (54). All constructs were transformed into *E. coli* BL21/DE3 by standard procedures (53).

Protein purification

Nine recombinant Mrp variants were expressed *in E. coli* BL21/DE3 cells transformed with pGEX4T1-*mrp* and purified *via* affinity chromatography. Single colonies of *E. coli* were cultured in LB media supplemented with Ap100 and grown overnight at 37 °C with agitation. The overnight cultures of stationary phase *E. coli* were inoculated into LB media and were grown at 37 °C with agitation until an absorbance (A_{600} nm) of 0.6 to 0.7 was reached. A final concentration of 0.1 mM isopropyl β-D-1-thiogalactopyranoside (Sigma-Aldrich) was added to the culture to induce the overexpression of Mrp in *E. coli*. Cultures were incubated at 30 °C for 4 h with agitation. Bacterial cells were pelleted by centrifugation (5000*g*, 10 min). Pellets were resuspended in ice-cold phosphate buffered saline (PBS) containing 1% Triton X-100 (Sigma-Aldrich). Cells were lysed using the Branson Sonifier 250 (Emerson) at 30% duty cycle with the microtip output control 2 for 2 min (10 s on, 10 s off) with 2 μg/ml DNase I (Sigma-Aldrich), 10 uM phenylmethylsulfonyl fluoride (Sigma-Aldrich), and 1 mg/ml lysozyme (Astral Scientific). The resulting lysate was rotated end over end for 30 min at 4 °C and centrifuged at 12,000*g* for 10 min to remove cellular debris. The supernatant was filtered using a 0.45 μM filter (Millipore). Filtered lysate was applied to a GST-agarose column (Sigma-Aldrich) with a bed volume of 1 ml. The column was then washed with PBS at 4 °C, and the protein was eluted with glutathione elution buffer (10 mM reduced glutathione (Sigma-Aldrich) in 50 mM Tris-HCl, pH 8.0). The eluted protein was incubated with 60 U of thrombin (Haematologic Technologies) for 4 h at room temperature to cleave GST tag from the recombinant Mrp. Cleaved protein was incubated with a 0.5 ml Ni-NTA column (Qiagen) for 1 h. The Ni-NTA column was then washed with PBS, and recombinant protein was eluted using native elution buffer (NaCl 17.5 g/L, NaH2PO4 6.9 g/L and Imidazole 17 g/L in MilliQ water). All steps of the purification process were analyzed by 12% sodium dodecyl sulphate polyacrylamide gel electrophoresis (SDS-PAGE), with protein visualized using Coomassie blue R250 staining on the Amersham AI600 (GE Healthcare). Precision Plus Protein Dual Color Standards marker (Bio-Rad) was used as a molecular weight marker to assess protein size and concentration.

Circular dichroism

Far-UV CD spectra were collected for recombinant Mrp to detect any potential differences in secondary structure using the Jasco J-810 Spectropolarimeter (Jasco). CD spectral data were continually recorded at room temperature from 180 to 250 nm in a 0.1 cm pathlength cell containing 400 μl of protein solution in 10 mM sodium phosphate buffer (pH 7.4). A continuous scanning mode was set, with a bandwidth of 1 nm, response time of 2 s and data pitch of 1. Data recorded represented the average of six scans, corrected for the buffer-only baseline. Molar residue ellipticity ([θ]) was calculated (55), and the data were plotted using GraphPad Prism, *version* 5 (GraphPad Software). To distinguish between coiled-coils and isolated helices, the 222:208 nm CD ratio was calculated as described previously (56). Additionally, BeStSel software (28) was used to deconvolute the Far-UV CD spectra

and obtain predictions of the relative abundance of different secondary structures in Mrp, including α-helix, β-strand, and turns.

Surface plasmon resonance

Binding interactions were analyzed using SPR on a BIAcore T200 (GE Healthcare). Recombinant 6x His-tagged Mrp were immobilized onto Series S Sensor Chip NTA (GE Healthcare) and binding to IgG (ab5608, Abcam), IgG1 (ab90283, Abcam), and IgG2 (ab90284, Abcam), IgG3 (ab118426, Abcam), and IgG4 (ab118426, Abcam) was determined at 25 °C on the BiacoreT200 *via* steady-state mode. All proteins and reagents were prepared in running buffer [PBS, 0.05% Tween-20 (Sigma-Aldrich), and 50 μM EDTA (Sigma-Aldrich) pH 7.4]. Flow cells 1, 2, 3, and 4 were activated with 0.5 mM NiCl2 (Sigma-Aldrich) at a 5 μl/min flow rate for 60s and washed with 3 mM EDTA at a 5 μl/min flow rate for 60 s. Assays were performed using analyte at varying concentrations over a series of seven separate injections for 2100 s at a flow rate of 5 μl/min followed by a 900 s dissociation period. IgG, IgG1, IgG2, and IgG4 were analyzed between 0 and 160 nM, and IgG3 was analyzed between 0 and 800 nM. The flow cell surface was regenerated twice between each analyte concentration with three steps: 500 mM imidazole (Sigma-Aldrich), 50 mM NaOH, and 350 mM EDTA (pH 8.3) for 30 s at a 100 μl/min flow rate. A steady-state affinity plot was used to determine the K_D of the interaction between Mrp and IgG. Data were analyzed *via* nonlinear fitting of sensograms according to a 1:1 Langmuir binding model in BIAevaluation, *version* 4.0.1 (Biacore AB) and plotted in GraphPad Prism *version* 5 (GraphPad Software). Data represent n = 3 ± SEM. A two-way ANOVA and Bonferroni post-test analysis of the K_D of all nine Mrp to IgG1, IgG2, IgG3, and IgG4 in GraphPad Prism, *version* 5 (GraphPad Software).

Plasma pulldown assay

Interactions between recombinant 6x His-tagged Mrp and IgG in human plasma were analyzed using pulldown assays. *E. coli* Bl21/DE3 cell lysates with enriched 6x His-tagged Mrp were prepared from cultures by the methods described above. Enriched Mrp lysates were incubated for 1 h at 25 °C or at 37 °C with 1:5 diluted human plasma, then purified from the plasma *via* NiNTA affinity chromatography (Qiagen). 4 to 20% Mini-PROTEAN TGX Stain-Free SDS-PAGE gels (Bio-Rad) were loaded with 8ug of total protein from the pooled elution fractions, and IgG was detected by immunoblotting onto PVDF membranes (Bio-Rad). Membranes were blocked for 1 h with 5% skim milk in Tris-buffered saline containing 0.1% (v/v) Tween 20 (TBST) and then incubated for an hour with 1:1000 mouse anti-6x His-tag antibody 27E8 (#2336, Cell Signaling Technology) for Mrp or with 1:1000 goat anti-human (H + L HRP conjugate) (#1721050, Bio-Rad) for IgG. Membranes were then washed thrice with TBST for 5 min between antibody incubations. Membranes incubated with the mouse anti-6x His-tag antibody were then incubated for 1 h at RT with 1:30,000 goat anti-mouse IgG conjugated with horseradish peroxidase (ab97023, Abcam). Blots were processed with Clarity Max Western ECL Blotting Substrate (Bio-Rad) and imaged with on the Amersham AI600 (GE Healthcare). BL21/DE3 *E coli* cells transformed with the empty vector (pGEX4T-1 vector backbone without Mrp) were also examined in the pulldown assay as a control and referred to as empty vector.

Mass photometry

The stoichiometry of Mrp: IgG was assessed using mass photometry. Samples containing Mrp216 and IgG at a 1:1, 1:10, and 10:1 M ratio in PBS (10ul of 100 nM Mrp216–10ul of 100 nM IgG) were prepared, and 10ul of each sample was analyzed over 10 min at a rate of 600 frames/min with an ONEMP mass photometer (Refeyn LTD). Mass photometry experiments were performed in duplicate. Data were obtained and analyzed using AquireMP and DiscoverMP, *version* 1.2.3 (Refeyn LTD) as previously described (57). M1 and M54 proteins were used as positive and negative controls, respectively.

Data availability

All data are contained in the figures, figure legends, or supporting material.

Supporting information—The article contains supporting information.

Acknowledgments—We thank Slobodan Jergic, Anuk Indraratna, Diane Ly, and Jonathan Williams for their technical support.

Author contributions—E. J. P., A. B., M. L. S-S., and P. S. conceptualization; E. J. P., H. F., J. G., P. S., M. D., S. S., and G. B. methodology; E. J. P., S. S., H. F., and J. U. investigation; E. J. P. writing-original draft; E. J. P formal analysis; M. L. S-S., M. D., P. S., D. D., J. G., J. M., S. S., H. F., and J. U. writing-reviewing and editing; M. L. S.-S. funding acquisition; M. L. S.-S., J. D. M., H. F., and M. D resources; M. L. S-S., J. G., and J. D. M. supervision.

Funding and additional information—This work was funded by NHMRC APP1143266 (M. L. S-S.). E. J. P. is a recipient of an Australian Postgraduate Award.

Conflict of interest—The authors declare they have no conflict of interest with the contents of this article.

Abbreviations—The abbreviations used are: CD, circular dichroism; Enn, M-like protein; IgG, immunoglobulin G; Mrp, M-related proteins; GAS, Group A *Streptococcus*/*Streptococcus pyogenes*; M, M protein; SPR, surface plasmon resonance.

References

1. Walker, M. J., Barnett, T. C., McArthur, J. D., Cole, J. N., Gillen, C. M., Henningham, A., *et al.* (2014) Disease manifestations and pathogenic mechanisms of group a Streptococcus. *Clin. Microbiol. Rev.* **27**, 264–301
2. Carapetis, J. R., Steer, A. C., Mulholland, E. K., and Weber, M. (2005) The global burden of group A streptococcal diseases. *Lancet Infect. Dis.* **5**, 685–694
3. Hondorp, E. R., and McIver, K. S. (2007) The Mga virulence regulon: infection where the grass is greener. *Mol. Microbiol.* **66**, 1056–1065

4. Frost, H. R., Davies, M. R., Delforge, V., Lakhloufi, D., Sanderson-Smith, M., Srinivasan, V., *et al.* (2020) Analysis of global collection of group A Streptococcus genomes reveals that the majority encode a Trio of M and M-like proteins. *mSphere* **5**, 2379–5042
5. Frost, H. R., Sanderson-Smith, M., Walker, M., Botteaux, A., and Smeesters, P. R. (2018) Group A streptococcal M-like proteins: from pathogenesis to vaccine potential. *FEMS Microbiol. Rev.* **42**, 193–204
6. Smeesters, P. R., McMillan, D. J., and Sriprakash, K. S. (2010) The streptococcal M protein: a highly versatile molecule. *Trends Microbiol.* **18**, 275–282
7. Vidarsson, G., Dekkers, G., and Rispens, T. (2014) IgG subclasses and allotypes: from structure to effector functions. *Front. Immunol.* **5**, 520
8. Jefferis, R., and Kumararatne, D. S. (1990) Selective IgG subclass deficiency: quantification and clinical relevance. *Clin. Exp. Immunol.* **81**, 357–367
9. Hammarström, L., and Smith, C. I. (1983) IgG2 deficiency in a healthy blood donor. Concomitant lack of IgG2, IgA and IgE immunoglobulins and specific anti-carbohydrate antibodies. *Clin. Exp. Immunol.* **51**, 600–604
10. Ferrante, A., Beard, L. J., and Feldman, R. G. (1990) IgG subclass distribution of antibodies to bacterial and viral antigens. *Pediatr. Infect. Dis. J.* **9**, S16–24
11. Aalberse, R. C., Stapel, S. O., Schuurman, J., and Rispens, T. (2009) Immunoglobulin G4: an odd antibody. *Clin. Exp. Allergy* **39**, 469–477
12. Courtney, H. S., and Li, Y. (2013) Non-immune binding of human IgG to M-related proteins confers resistance to phagocytosis of group A streptococci in blood. *PLoS One* **8**, 78719
13. Cedervall, T., Akesson, P., Stenberg, L., Herrmann, A., and Akerstom, B. (1995) Allosteric and temperature effects on the plasma protein binding by streptococcal M protein family members. *Scand. J. Immunol.* **42**, 433–441
14. Gubbe, K., Misselwitz, R., Welfle, K., Reichardt, W., Schmidt, K. H., and Welfle, H. (1997) C repeats of the streptococcal M1 protein achieve the human serum albumin binding ability by flanking regions which stabilize the coiled-coil conformation. *Biochemistry* **36**, 8107–8113
15. Akerström, B., Lindahl, G., Björck, L., and Lindqvist, A. (1992) Protein Arp and protein H from group A streptococci. Ig binding and dimerization are regulated by temperature. *J. Immunol.* **148**, 3238–3243
16. Cedervall, T., Johansson, M. U., and Akerström, B. (1997) Coiled-coil structure of group A streptococcal M proteins. Different temperature stability of class A and C proteins by hydrophobic-nonhydrophobic amino acid substitutions at heptad positions a and d. *Biochemistry* **36**, 4987–4994
17. Nilson, B. H. K., Frick, I.-M., Aakesson, P., Forsen, S., Bjoerck, L., Aakerstroem, B., *et al.* (1995) Structure and stability of protein H and the M1 protein from Streptococcus pyogenes. Implications for other surface proteins of Gram-positive bacteria. *Biochemistry* **34**, 13688–13698
18. Stewart, C. M., Buffalo, C. Z., Valderrama, J. A., Henningham, A., Cole, J. N., Nizet, V., *et al.* (2016) Coiled-coil destabilizing residues in the group A Streptococcus M1 protein are required for functional interaction. *Proc. Natl. Acad. Sci. U. S. A.* **113**, 9515
19. Heath, D. G., Boyle, M. D., and Cleary, P. P. (1990) Isolated DNA repeat region from fcrA76, the Fc-binding protein gene from an M-type 76 strain of group A streptococci, encodes a protein with Fc-binding activity. *Mol. Microbiol.* **4**, 2071–2079
20. Stenberg, L., O'Toole, P., and Lindahl, G. (1992) Many group A streptococcal strains express two different immunoglobulin-binding proteins, encoded by closely linked genes: characterization of the proteins expressed by four strains of different M-type. *Mol. Microbiol.* **6**, 1185–1194
21. O'Toole, P., Stenberg, L., Rissler, M., and Lindahl, G. (1992) Two major classes in the M protein family in group A streptococci. *Proc. Natl. Acad. Sci. U. S. A.* **89**, 8661–8665
22. Li, Y., and Courtney, H. S. (2011) Promotion of phagocytosis of Streptococcus pyogenes in human blood by a fibrinogen-binding peptide. *Microbes Infect.* **13**, 413–418
23. Davies, M. R., McIntyre, L., Mutreja, A., Lacey, J. A., Lees, J. A., Towers, R. J., *et al.* (2019) Atlas of group A streptococcal vaccine candidates compiled using large-scale comparative genomics. *Nat. Genet.* **51**, 1035–1043
24. Frost, H. R., Guglielmini, J., Duchêne, S., Lacey, J. A., Sanderson-Smith, M., Steer, A. C., *et al.* (2023) Promiscuous evolution of group A streptococcal M and M-like proteins. *Microbiology (Reading)* **169**, 001280
25. Sanderson-Smith, M., De Oliveira, D. M., Guglielmini, J., McMillan, D. J., Vu, T., Holien, J. K., *et al.* (2014) A systematic and functional classification of Streptococcus pyogenes that serves as a new tool for molecular typing and vaccine development. *J. Infect. Dis.* **210**, 1325–1338
26. Frost, H. R. (2020) *Characterisation of the Group A Streptococcus M and M-Like Proteins as Potential Vaccine Antigens*. PhD, Université Libre de Bruxelles
27. Kwok, S. C., and Hodges, R. S. (2004) Stabilizing and destabilizing clusters in the hydrophobic core of long two-stranded alpha-helical coiled-coils. *J. Biol. Chem.* **279**, 21576–21588
28. Micsonai, A., Moussong, É., Wien, F., Boros, E., Vadászi, H., Murvai, N., *et al.* (2022) BeStSel: webserver for secondary structure and fold prediction for protein CD spectroscopy. *Nucleic Acids Res.* **50**, W90–W98
29. Khakzad, H., Happonen, L., Karami, Y., Chowdhury, S., Bergdahl, G. E., Nilges, M., *et al.* (2021) Structural determination of Streptococcus pyogenes M1 protein interactions with human immunoglobulin G using integrative structural biology. *PLoS Comput. Biol.* **17**, e1008169
30. Akesson, P., Schmidt, K. H., Cooney, J., and Björck, L. (1994) M1 protein and protein H: IgGFc- and albumin-binding streptococcal surface proteins encoded by adjacent genes. *Biochem. J.* **300**, 877–886
31. Stenberg, L., O'Toole, P. W., Mestecky, J., and Lindahl, G. (1994) Molecular characterization of protein Sir, a streptococcal cell surface protein that binds both immunoglobulin A and immunoglobulin G. *J. Biol. Chem.* **269**, 13458–13464
32. Åkesson, P., Conney, J., Kishimoto, F., and Björck, L. (1990) Protein H–a novel IgG binding bacterial protein. *Mol. Immunol.* **27**, 523–531
33. Ermert, D., Laabei, M., Weckel, A., Mörgelin, M., Lundqvist, M., Björck, L., *et al.* (2019) The molecular basis of human IgG-mediated enhancement of C4b-binding protein recruitment to group A Streptococcus. *Front. Immunol.* **10**, 1230
34. Pack, T. D., Podbielski, A., and Boyle, M. D. P. (1996) Identification of an amino acid signature sequence predictive of protein G-inhibitable IgG3-binding activity in group-A streptococcal IgG-binding proteins. *Gene* **171**, 65–70
35. McNamara, C., Zinkernagel, A. S., Macheboeuf, P., Cunningham, M. W., Nizet, V., and Ghosh, P. (2008) Coiled-coil irregularities and instabilities in group A Streptococcus M1 are required for virulence. *Science (New York, N.Y.)* **319**, 1405–1408
36. Mills, J. O., and Ghosh, P. (2021) Nonimmune antibody interactions of Group A Streptococcus M and M-like proteins. *PLoS Pathog.* **17**, e1009248
37. Bessen, D. E., Izzo, M. W., McCabe, E. J., and Sotir, C. M. (1997) Two-domain motif for IgG-binding activity by group A streptococcal emm gene products. *Gene* **196**, 75–82
38. Podbielski, A. (1993) Three different types of organization of the vir regulon in group A streptococci. *Mol. Gen. Genet.* **237**, 287–300
39. Hollingshead, S. K., Readdy, T. L., Yung, D. L., and Bessen, D. E. (1993) Structural heterogeneity of the emm gene cluster in group A streptococci. *Mol. Microbiol.* **8**, 707–717
40. Nordenfelt, P., Waldemarson, S., Linder, A., Mörgelin, M., Karlsson, C., Malmström, J., *et al.* (2012) Antibody orientation at bacterial surfaces is related to invasive infection. *J. Exp. Med.* **209**, 2367–2381
41. Herwald, H., Cramer, H., Mörgelin, M., Russell, W., Sollenberg, U., Norrby-Teglund, A., *et al.* (2004) M protein, a classical bacterial virulence determinant, forms complexes with fibrinogen that induce vascular leakage. *Cell* **116**, 367–379
42. Berge, A., and Björck, L. (1995) Streptococcal cysteine proteinase releases biologically active fragments of streptococcal surface proteins. *J. Biol. Chem.* **270**, 9862–9867
43. Sjöholm, K., Karlsson, C., Linder, A., and Malmström, J. (2014) A comprehensive analysis of the Streptococcus pyogenes and human plasma protein interaction network. *Mol. BioSystems* **10**, 1698–1708

44. Heath, D. G., and Cleary, P. P. (1987) Cloning and expression of the gene for an immunoglobulin G Fc receptor protein from a group A streptococcus. *Infect. Immun.* **55**, 1233–1238
45. Podbielski, A., Schnitzler, N., Beyhs, P., and Boyle, M. D. (1996) M-related protein (Mrp) contributes to group A streptococcal resistance to phagocytosis by human granulocytes. *Mol. Microbiol.* **19**, 429–441
46. Pack, T. D., and Boyle, M. D. (1995) Characterization of a type II'o group A streptococcal immunoglobulin-binding protein. *Mol. Immunol.* **32**, 1235–1243
47. Damelang, T., Rogerson, S. J., Kent, S. J., and Chung, A. W. (2019) Role of IgG3 in infectious diseases. *Trends Immunol.* **40**, 197–211
48. Diebolder, C. A., Beurskens, F. J., de Jong, R. N., Koning, R. I., Strumane, K., Lindorfer, M. A., *et al.* (2014) Complement is activated by IgG hexamers assembled at the cell surface. *Science (New York, N.Y.)* **343**, 1260–1263
49. Brüggemann, M., Williams, G. T., Bindon, C. I., Clark, M. R., Walker, M. R., Jefferis, R., *et al.* (1987) Comparison of the effector functions of human immunoglobulins using a matched set of chimeric antibodies. *J. Exp. Med.* **166**, 1351–1361
50. Whatmore, A. M., Kapur, V., Musser, J. M., and Kehoe, M. A. (1995) Molecular population genetic analysis of the enn subdivision of group A streptococcal emm-like genes: horizontal gene transfer and restricted variation among enn genes. *Mol. Microbiol.* **15**, 1039–1048
51. Dale, J. B., Niedermeyer, S. E., Agbaosi, T., Hysmith, N. D., Penfound, T. A., Hohn, C. M., *et al.* (2015) Protective immunogenicity of group A streptococcal M-related proteins. *Clin. Vaccin. Immunol.* **22**, 344–350
52. Lupas, A., Van Dyke, M., and Stock, J. (1991) Predicting coiled coils from protein sequences. *Science (New York, N.Y.)* **252**, 1162
53. Sambrook, J., Fritsch, E., and Maniatis, T. (1989) *Molecular Cloning. A Laboratory Manual*, 2nd edn., Cold Spring Harbor Laboratory Press, New York
54. Podbielski, A., Hawlitzky, J., Pack, T. D., Flosdorff, A., and Boyle, M. D. (1994) A group A streptococcal Enn protein potentially resulting from intergenomic recombination exhibits atypical immunoglobulin-binding characteristics. *Mol. Microbiol.* **12**, 725–736
55. Greenfield, N. J. (2006) Using circular dichroism spectra to estimate protein secondary structure. *Nat. Protoc.* **1**, 2876–2890
56. Batchelor, M., Wolny, M., Kurzawa, M., Dougan, L., Knight, P. J., and Peckham, M. (2018) Determining stable single alpha helical (SAH) domain properties by circular dichroism and atomic force microscopy. *Methods Mol. Biol. (Clifton, N.J.)* **1805**, 185–211
57. Cole, D., Young, G., Weigel, A., Sebesta, A., and Kukura, P. (2017) Label-free single-molecule imaging with numerical-aperture-shaped interferometric scattering microscopy. *ACS Photon.* **4**, 211–216